



1   **MODIFICATIONS    TO    KOZENY-CARMAN    MODEL    To**  
2   **ENHANCE PETROPHYSICAL RELATIONSHIPS**

3   Amir Maher Sayed Lala

4   Geophysics Department, Ain Shams University

5   **e-mail: [amir77\\_lala@yahoo.com](mailto:amir77_lala@yahoo.com)**

6   **Affiliation:** Geophysics Department, Fac. of Science, Ain Shams University

7

8

9

10

11

12

13

14

15

16

17

18

19

20

21

22



## 23 MODIFICATIONS TO KOZENY-CARMAN EQUATION To 24 ENHANCE PETROPHYSICAL RELATIONSHIPS

25 Amir M. S. Lala

26 Geophysics Department, Ain Shams University

## Abstract

28 The most commonly used relationship relates permeability to porosity, grain  
29 size, and tortuosity is Kozeny-Carman formalism. When it is used to estimate the  
30 permeability behavior versus porosity, the other two parameters (the grain size and  
31 tortuosity) are usually kept constant. Here, we investigate the deficiency of the  
32 Kozeny-Carman assumption and offer alternative derived equations for the Kozeny-  
33 Carman equation, including equations where the grain size is replaced with the pore  
34 size and with varying tortuosity. We also introduced relationships for the permeability  
35 of shaly sand reservoir that answer the approximately linear permeability decreases in  
36 the log-linear permeability-porosity relationships in datasets from different locations.

37

## Introduction

39 Darcy's law (e.g., Mavko et al., 2009) states that, the volume flux of viscous  
40 fluid  $Q$  (volume per time unit, e.g.,  $\text{m}^3/\text{s}$ ) through a sample of porous material is  
41 proportional to the cross-sectional area  $A$  and the pressure difference  $\Delta P$  applied to  
42 the sample's opposite faces, and inversely proportional to the sample length  $L$  and the  
43 fluid's dynamic viscosity  $\mu$ , as shown as follows :

45 The proportionality constant  $k$  is called the absolute permeability. The main  
 46 assumption of Darcy's law is that,  $k$  does not depend on the fluid viscosity  $\mu$  or  
 47 pressure difference  $\Delta P$ . All inputs in equation 1 have to have consistent units,



meaning that if length is in m, pressure has to be in Pa and viscosity in Pa s. The most commonly used viscosity unit is cPs =  $10^{-3}$  Pa s. It follows from Equation 1 that the units of  $k$  are length squared, e.g., m<sup>2</sup>. The most common permeability units used in the industry are Darcy (D) and/or milliDarcy (mD): 1D =  $10^{-12}$  m<sup>2</sup> and 1 mD =  $10^{-15}$  m<sup>2</sup>.

53 The Kozeny-Carman (KC) formalism (e.g., Mavko et al., 2009) assumes that a  
 54 porous solid can be represented as a solid block permeated by parallel cylindrical  
 55 pores (pipes) whose axes may be at an angle to the direction of the pressure gradient,  
 56 so that the length of an individual pipe is larger than that of the block. To relate  
 57 permeability to porosity in such idealized porous solid we need to find how the  
 58 volume flux  $Q$  relates to the pressure gradient  $\Delta P$ . The solution is based on the  
 59 assumption that each cylindrical pipe is circular, with radius  $r$ . The Navier-Stokes  
 60 equations governing laminar viscous flow through a circular pipe of radius  $r$  provide  
 61 the following expression for the volume flux  $q$  through an individual pipe:

62

64

65 where:  $l$  is the length of the pipe.

66 Our derivation starts from the Kozeny-Carman equation by assuming that a  
 67 rock includes porosity of pipe shape. Permeability of this rock is expressed by its  
 68 porosity  $\phi$  and the specific surface area  $S$  to the radius of an individual pipe, its  
 69 length, and the number of the pipes, and using Equation 1, we get:



71 where:  $S$  is defined as the ratio of the total pore surface to the total volume of the  
72 porous sample and the tortuosity  $\tau$  is simply  $1 / L$ , defined as the ratio of the length of  
73 the fluid path to that of the sample. Porosity can be evaluated in the laboratory or  
74 obtained from porosity logs. The specific surface area is much more difficult to  
75 measure or infer. One other parameter that can be determined in the laboratory is the  
76 average grain size (diameter)  $d$ . This is why it is possible to conduct relationship  
77 between  $k$  and  $d$ . So modified Kozeny– Carman equation is needed if a non-fractal  
78 spherical grain packing model is assumed (yielding a constant tortuosity) and the  
79 effective pore radius is substituted by a term involving the specific surface expressed  
80 by the grain radius and the porosity. This operation is inconsistent with the KC  
81 formalism but it is useful. Assume that the number of these grains is  $n$ , their volume is  
82  $n\pi d^3 / 6$  while their surface area is  $n\pi d^2$ . Because the grains occupy the volume  
83 fraction  $1-\varphi$  of the entire rock, the total volume of the rock is  $n\pi d^3 / 6(1-\varphi)$ . As a  
84 result, the specific surface area is  $6(1-\varphi) / d$ .

85 By replacing  $S$  in equation 3 with the latter expression, we find:

87 which is a commonly used form of KC equation. The units used in this equation have  
 88 to be consistent. In practical use they are often not, meaning that  $d$  is measured in mm  
 89 while  $k$  is in mD. For these units, equation 4 can be read as:

91 Mavko and Nur (1997) modified this equation by introducing the percolation porosity  
92  $\varphi_p$  below which the pore space becomes disconnected and  $k$  becomes zero, although  $\varphi$   
93 is still finite;



95 where, as before,  $k$  is in mD,  $d$  is in mm, and  $\varphi$  is in fraction of one.

## 96 Kozeny-Carman Equation with Pore Size

As we discussed in the introduction, using the grain size in KC equation is not consistent with the formalism where the pore space is idealized as a set of parallel pipes.

Let us explore whether we can introduce the length parameter into KC equation in a more logical way and reformulate it using the pore size rather than grain size. With this goal in mind, let us recall another form of KC equation (e.g., Mavko et al., 2009)

105 where  $r$  is the radius of the circular pipe that passes through the solid block and  $D$  is  
106 its diameter.

Let us assume, hence, that the porosity only depends on the size of the pipe and is proportional to its cross-section, i.e., proportional to  $D^2$ . Hence, if the pore's diameter is  $D_0$  at porosity  $\phi_0$  and  $D$  at porosity  $\phi$ ,

111 As a result, by combining Equations (7) and (8), we obtain:

113 This equation relates the permeability to porosity squared rather than cubed, the latter  
114 as in more common forms of the KC equation. As a result, if in equation 9 we assume  
115  $\tau$  constant, the permeability reduction due to reducing porosity will be much less  
116 pronounced than exhibited by the Rudies data and the respective theoretical curves



117 will strongly overestimate the permeability data. To mitigate this effect, let us assume  
 118 that the tortuosity is not constant but rather changes with porosity.

119 The tortuosity is an idealized parameter that has a clear meaning within the  
120 KC formalism but becomes fairly nebulous in a realistic pore space that is not made of  
121 parallel cylindrical pipes. Still, numerous authors discussed the physical meaning of  
122 tortuosity in real rock, designed experimental and theoretical methods of obtaining it,  
123 and suggested that  $\tau$  could be variable (even within the same dataset) as a function of  
124 porosity.

125 Let us focus here on two tortuosity equations:

127 That is derived from laboratory contaminant diffusion experiments by Boving and  
128 Grathwohl  
129 (2001) and

131 That is theoretically derived by Berryman (1981).

132

At  $\varphi = 0.3$ , these two equations give  $\tau = 4.24$  and  $2.17$ , respectively. Because KC with  $\tau = 2.50$  matches the laboratory Rudies data at  $\varphi = 0.3$ , let us modify equations 10 and 11 so that both produce  $\tau = 2.50$  at  $\varphi = 0.3$ . These equations thus modified become, respectively,

138 and

140 By substituting equations 12 and 13 into equation 9, we arrive at the following  
141 two KC estimates, respectively:



143 and

145 with equation 14 giving the lower permeability estimate and equation 15 giving the  
146 upper estimate for porosity below 30%. For permeability in mD and pore diameter in  
147 mm, a multiplier  $10^9$  has to be added to the right-hand sides of these equations.

148 Finally, by introducing the percolation porosity into these equations and using  
 149 the units  $mD$  for  $k$  and  $mm$  for  $D_0$ , we obtain, respectively,

$$k = 0.0898 \times 10^9 \frac{D_0^2}{\varphi_0} (\varphi - \varphi_p)^{4.4} \quad \dots \dots \dots \quad (16)$$

151 and

153

154 Other Permeability-Porosity Trends and Their Explanation

155 In most rocks, permeability does not follow the classic clay free trend  
156 equations 16 and 17. The question is then how to use the KC equation to explain or  
157 predict permeability in such formations. To address this question, we will use the KC  
158 functional form with the grain size  $d$ .

159 Let us now recall equation 3 and modify it to be used with  $k$  in mD and  $S$  in  
160  $\text{mm}^{-1}$ :

162 Assume next that the porosity evolution is due to mixing of two distinctively  
 163 different grain sizes. The larger grain size is  $d_{ss}$  while the smaller grain size is  $d_{sh}$  and



164  $d_{sh} = \lambda d_{ss}$  ..... (19)

165 where:  $\lambda < 1$  is constant.

166 Let the volume fraction of the smaller grains in the rock be  $C$  (we call it the  
 167 shale content). Then, by following Marion's (1990) formalism and assuming grain  
 168 mixing according to the ideal binary scheme (Figure 6), we obtain the total porosity  $\varphi$   
 169 of this mixture as shown:

170  $\varphi = \varphi_{ss} - C(1 - \varphi_{sh})$  ..... (20)

171 for  $C \leq \varphi_{ss}$ , where  $\varphi_{ss}$  is the porosity of the large grain framework while  $\varphi_{sh}$  is that of  
 172 the small grain framework.

173 Recalling now the expression for the specific surface area given earlier in the  
 174 text, we obtain for the large grain framework (sand)

175  $S_{ss} = \frac{6(1 - \varphi_{ss})}{d_{ss}}$  ..... (21)

176 and for the shale

177  $S_{sh} = \frac{6(1 - \varphi_{sh})}{d_{sh}}$  ..... (22)

178 Assume next that the total specific surface area of the sand/shale mixture is the  
 179 sum of the two, the latter is weighted by the shale content:

180  $S = S_{ss} + CS_{sh} = \frac{6}{d_{ss}} [1 - \varphi_{ss} + C(1 - \varphi_{ss})/\lambda]$  ..... (23)

181 Now, by using Equations 20 and 23 together with equation 18, we find:

182  $k = \frac{10^9 d_{ss}^2}{72 \tau^2} \frac{[\varphi_{ss} - C(1 - \varphi_{sh})]^3}{[1 - \varphi_{ss} + C(1 - \varphi_{ss})/\lambda]^2}$  ..... (24)

183 As before, we can modify equation 24 to include the percolation porosity:

184  $k = \frac{10^9 (\varphi - \varphi_p)^3}{2 S^2 \tau^2} = \frac{10^9 d_{ss}^2 [\varphi_{ss} - C(1 - \varphi_{sh}) - \varphi_p]^3}{72 \tau^2 [1 - \varphi_{ss} + C(1 - \varphi_{ss})/\lambda]^2}$  ..... (25)

185 where the total porosity is, as before,  $\varphi = \varphi_{ss} - C(1 - \varphi_{sh})$ .



186

## Results and Discussion

187 An example of using equation (6) to mimic the Rudies sandstone data (Lala,  
188 2003) as well as the sorted Matullah sand data obtained from Belayim marine field,  
189 Gulf of Suez, Egypt is shown in Figure 1. The curve in this figure is according to  
190 Equation 6 with  $d = 0.250$  mm (for Rudies),  $\tau = 2.5$ , and  $\varphi_p = \text{zero}, 0.01, 0.02$ , and  
191 0.03. The grain size in the Matullah dataset varies between 0.115 and 0.545 mm.

192

193 The Figure 2 shows the permeability normalized by the grain size squared,  $d^2$ .  
194 The Rudies sand data trend retains its shape. However, the Matullah sand data now  
195 form a distinct permeability-porosity trend which approximately falls on the KC  
196 theoretical curve. This fact emphasizes the effect of the grain size on the permeability  
197 in obtaining permeability-porosity trends for formations where  $d$  is variable,  $k / d^2$   
198 rather than  $k$  alone is the appropriate argument.

199

200 Notice that although Equation 6 with  $\varphi_p > 0$  mimics the permeability-porosity  
201 behavior of Rudies Formation data at high and low porosity, it somewhat  
202 underestimates the permeability in the 0.10 to 0.20 porosity range. The  $\varphi_p = 0$  curve  
203 matches the data for porosity above 0.10 but overestimates the permeability in the  $\varphi <$   
204 0.10 range. This is why in this porosity range, Bourbie et al. (1987) suggested to use a  
205 higher power of  $\varphi$  (e.g., 8) instead of 3. To us, introducing a finite percolation  
206 porosity appears to be more physically meaningful. Still, no matter how we choose to  
207 alter the input parameters, it is important to remember that KC equation is based on  
208 highly idealized representations of the pore space and it is remarkable that it  
209 sometimes works (same has to be said about two other remarkable “guesses.”



210 Archie's law for the electrical resistivity and Raymer's equation for the P-wave  
211 velocity, both discussed in Mavko et al., 2009).

212 Also, by observing the pore-space geometry evolution in Rudies sandstone,  
213 one may conclude that the pore size is variable (Figure 3): the pores shrink with  
214 decreasing porosity. In such a reservoir, the predicted permeability would be perfect if  
215 we consider only the porosity (pore spaces) and grain size in prediction.

216 The resulting tortuosity from equations 12 & 13 plotted versus porosity in  
217 Figure 4 rapidly increases with decreasing porosity, especially so in the porosity range  
218 below 10%.

219 Let us assume that  $\varphi_o = 0.30$ ,  $D_0 = 0.10$  mm, and  $\varphi_p = 0.01$ . The respective curves  
220 according to the two equations 16 & 17 are plotted on top of the Rudies and Mutallah  
221 data in Figure 5.

222 The percolation porosity used here is different from 0.02 used in Equation 6.  
223 The reason is that the current value 0.01 in Equations 16 and 17 gives a better match  
224 to Rudies data in the lower porosity range.

225 Needless to say that, the concept of "pore size" is a strong idealization, same  
226 as the concept of "grain size." We introduced it here because it is more consistent  
227 with the KC formalism than the latter idealization. Practical reason for using the  
228 equations with pore size is that this parameter can be inferred from the mercury  
229 injection experiments or directly from a digital image of a rock sample.

230 Let us assume  $d_{ss} = 0.25$  mm;  $\tau = 2.5$  (fixed); and  $\varphi_{ss} = \varphi_{sh} = 0.36$ . The  
231 resulting theoretical permeability estimates from equation 24 are plotted versus  
232 porosity in Figure 6 for  $\lambda = 1.00$ ; 0.10 ;and 0.01.

233 The curve for  $\lambda = 0.10$  matches the Kharita Member data trend, obtained from  
234 the Western Desert, Egypt, while that for  $\lambda = 0.01$  matches the Bahariya Formation



235 data trend (Lala & Nahla, 2014). The curve for  $\lambda = 1.00$  matches the high porosity  
236 part of the Rudies Formation data trend.

237 The percolation porosity value only weakly affects the theoretical permeability  
238 curves in the high and middle porosity ranges. This is why in Figure 6 we only show  
239 curves with  $\varphi_p = 0$ .

#### 240 Conclusion

241 The goal of this work is to explore permutations of the Kozeny-Carman  
242 formalism and derive respective equations. Although the idealizations used in these  
243 derivations are strong and sometimes lack internal consistency, the results indicate the  
244 significant flexibility of this formalism. The variants of the KC equation shown here  
245 can explain the various permeability-porosity trends observed in the laboratory,  
246 sometimes within the framework of physical and geological reasoning. The predictive  
247 ability of these equations is arguable since the input constants are not necessarily a-  
248 priori known. Still, as in the case of bimodal mixtures, they can help with the quality  
249 control of the existing data and forecasting of the permeability-porosity trends in  
250 similar sedimentary textures.

251

252

253

#### 254 Acknowledgments

255 The author is indebted to the Egyptian General Petroleum Corporation  
256 (EGPC) for the permission to publish these laboratory results. The author is also  
257 grateful to anonymous reviewers whose constructive comments helped to improve  
258 this manuscript.



## References

Amir, M.S. Lala, 2003, Effect of Sedimentary Rock Textures and Pore Structures on Its Acoustic Properties, M.Sc. Thesis, Geophysics Department, Ain Shams University, Egypt.

Amir, M.S. Lala, and Nahla, A.A. El-Sayed, 2015, The application of petrophysics to resolve fluid flow units and reservoir quality in the Upper Cretaceous Formations: Abu Sennan oil field, Egypt, Journal of African Earth Sciences, 102.

Berryman, J.G., 1981, Elastic wave propagation in fluid-saturated porous media, Journal of Acoustical Society of America, 69, 416-424.

Blangy, J. P., 1992, Integrated seismic lithologic interpretation: The petrophysical basis, Ph.D. thesis, Stanford University.

Bourbie, T., O. Coussy, and B. Zinszner, 1987, Acoustics of porous media, Gulf Publishing Company.

Boving, T.B., and Grathwohl, P., 2001, Tracer diffusion coefficients in sedimentary rocks: correlation to porosity and hydraulic conductivity, Journal of Contaminant Hydrology, 53, 85-100.

Marion, D., 1990, Acoustical, mechanical and transport properties of sediments and granular materials, Ph.D. thesis, Stanford University.

Mavko, G., and Nur, A., 1997, The effect of a percolation threshold in the Kozeny-Carman relation, Geophysics, 62, 1480-1482.

Mavko, G., Mukerji, T., and Dvorkin, J., 2009, The rock physics handbook, Cambridge University press.



Strandenes, S., 1991, Rock physics analysis of the Brent Group Reservoir in the Oseberg Field, Stanford Rock Physics and Borehole Geophysics Project, special volume.

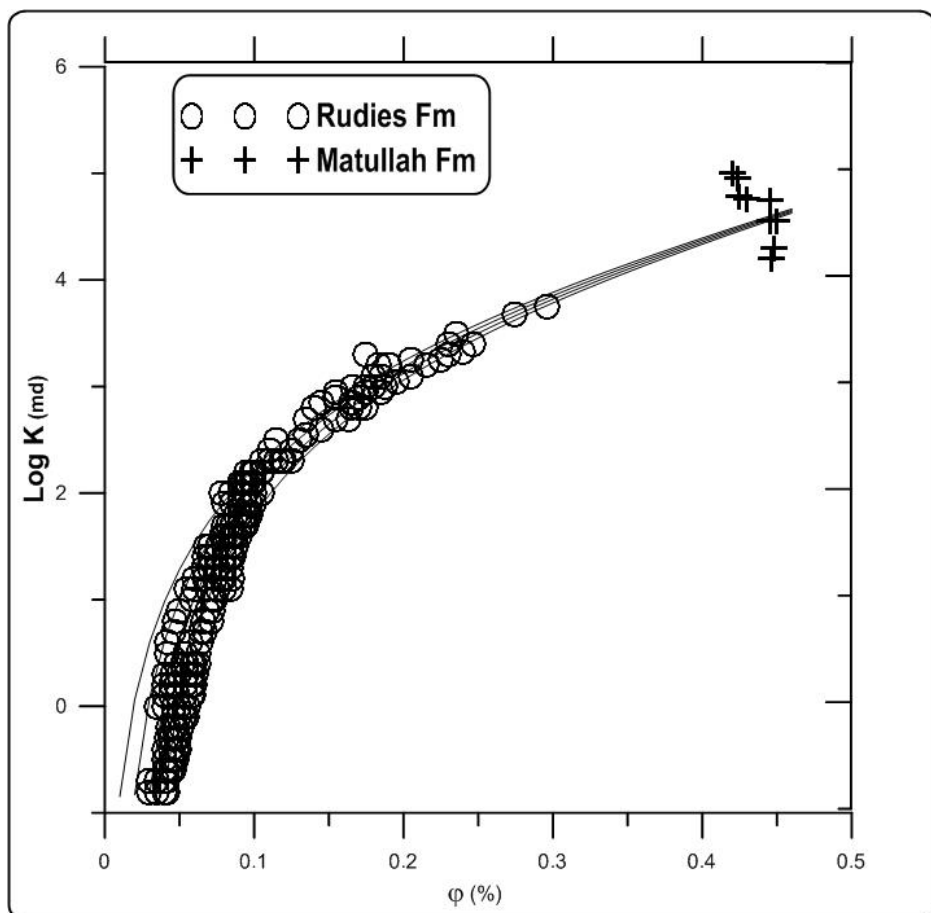


**Fig.1.** Porosity vs Permeability, the curves are from equation 6 with the percolation porosity (uppermost curve), 0.01, 0.02 and 0.03 (lowermost curve).

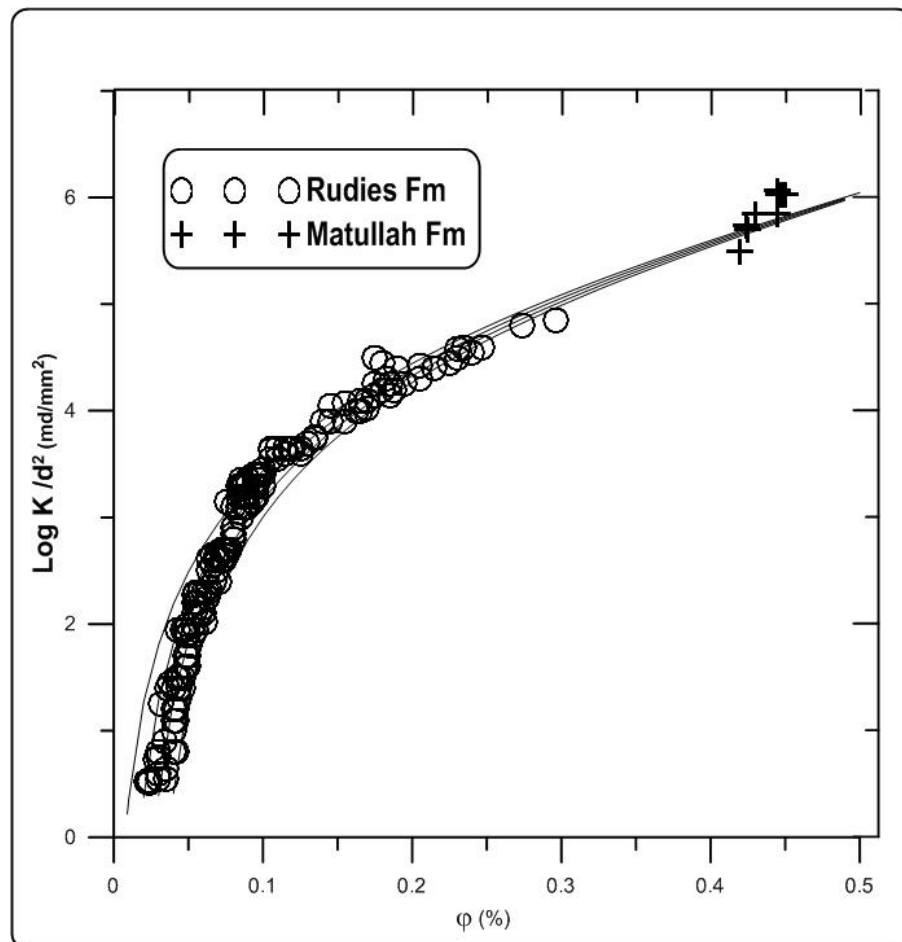


**Fig.2.**Porosity vs Permeability normalized by the grain size squared, the curves are from equation 6.

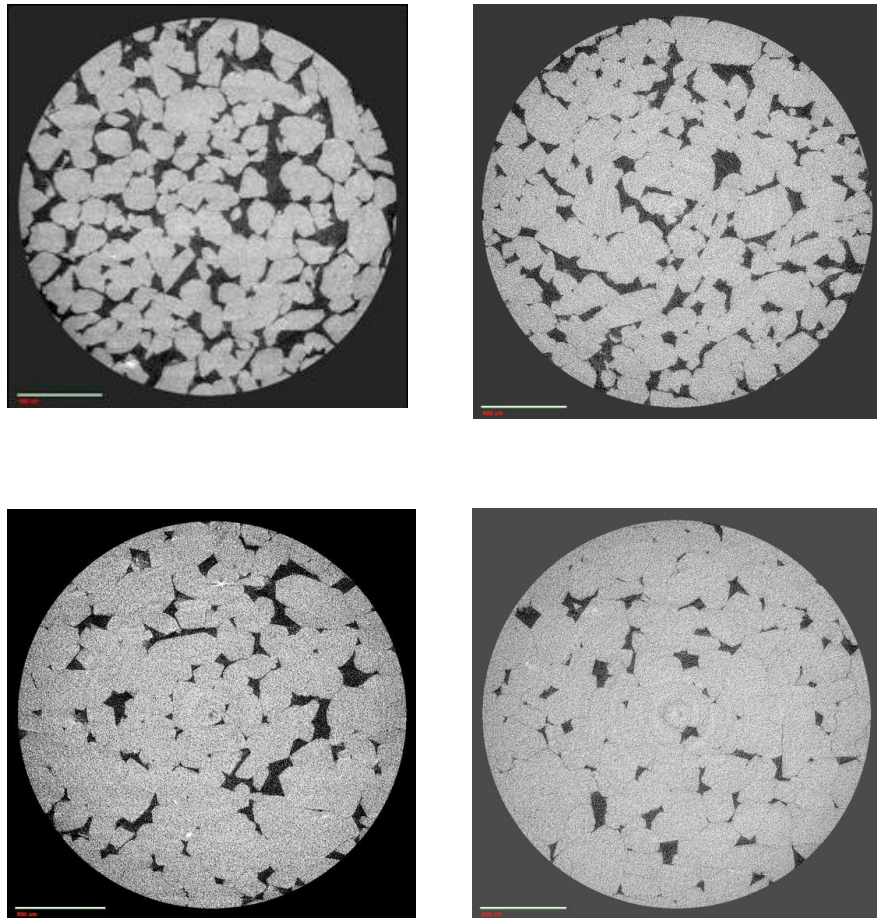
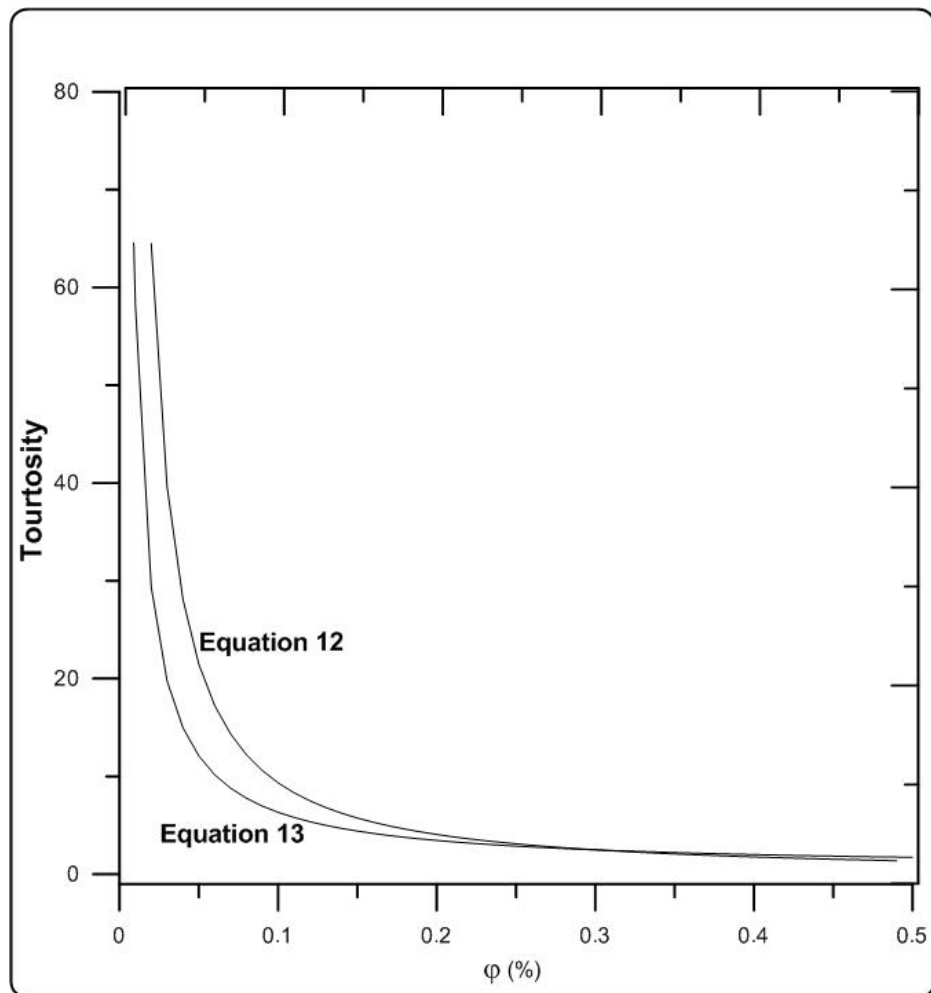
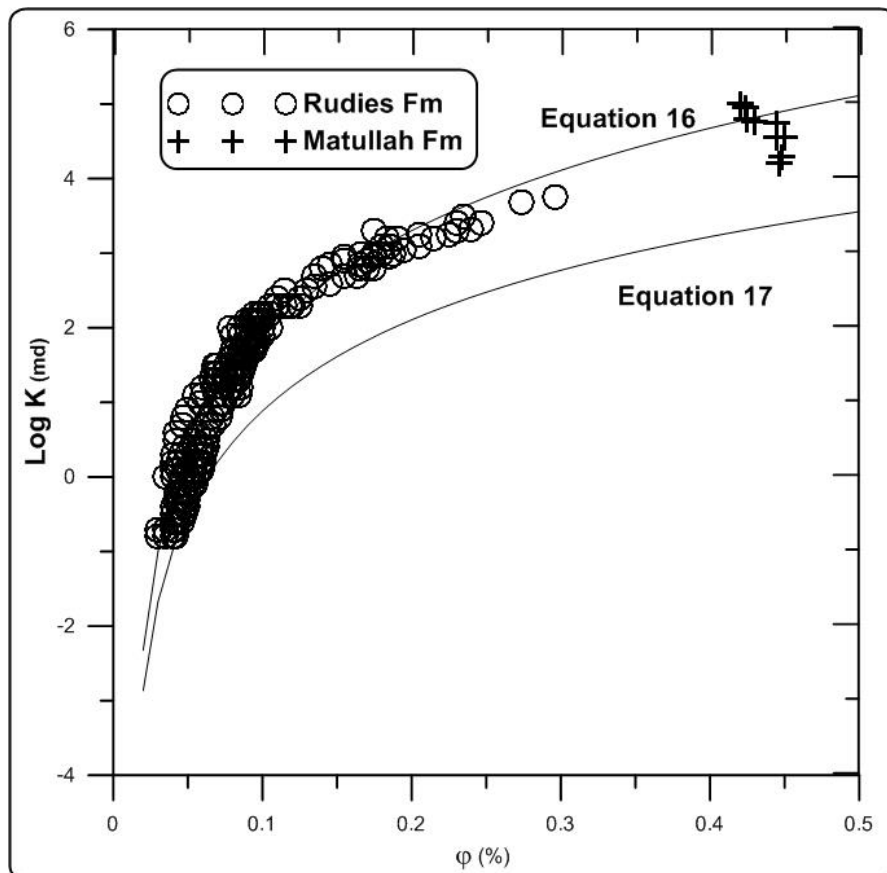


Fig.3. digital slice through four Rudies Fm samples whose porosity is gradually reducing (left to right and top to bottom). The scale bar in each image is 500 $\mu$ m.



**Fig.4. Porosity versus Tourtosity.**



**Fig.5.**Porosity versus Permeability, curves are from equation 16 and 17.

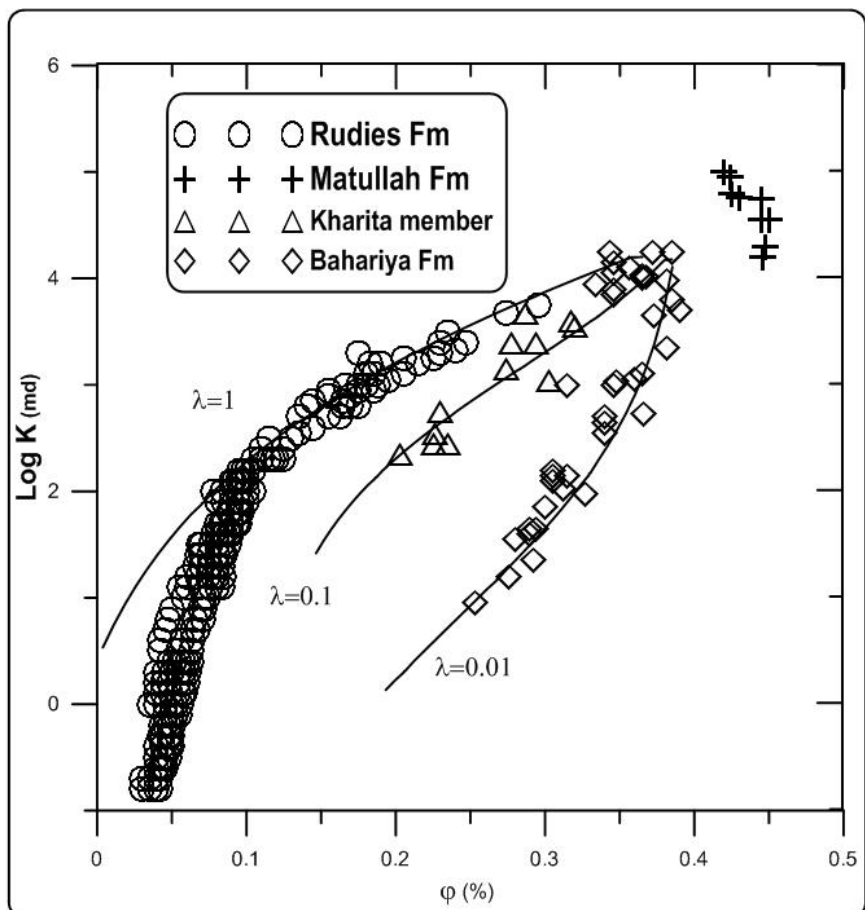


**Fig.6.**Porosity vs Permeability, the curves are from equation 24.